The QCD phase diagram: A comparison of lattice and hadron resonance gas model calculations

A. Taw k

University of Bielefeld, P.O. Box 100131, D-33501 Bielefeld, Germany

(D ated: 23. D ecem ber 2004)

Abstract

We compare the lattice results on QCD phase diagram for two and three—avors with the hadron resonance gas model (HRGM) calculations. Lines of constant energy density—have been determined at different baryo-chemical potentials $_{\rm B}$. For the strangeness chemical potentials $_{\rm S}$, we use two models. We explicitly set $_{\rm S}=0$ for all temperatures and baryo-chemical potentials. This assignment is used in lattice calculations. In the other model, $_{\rm S}$ is calculated in dependence on T and $_{\rm B}$ according to the condition of vanishing strangeness. We also derive an analytical expression for the dependence of $T_{\rm C}$ on $_{\rm B}$ =T by applying Taylor expansion of . In both cases, we compare HRGM results on $T_{\rm C}$ $_{\rm B}$ diagram with the lattice calculations. The agreement is excellent, especially when the trigonometric function of is truncated up to the same order as done in lattice simulations. For studying the eleciency of the truncated Taylor expansion, we calculate the radius of convergence. For zero—and second—order radii, the agreement with lattice is convincing. Furthermore, we make predictions for QCD phase diagram for non-truncated expressions and physical masses. These predictions are to be conorm med by heavy—ion experiments and fiture lattice calculations with very small lattice spacing and physical quark masses.

PACS numbers: 1238Gc, 2410Pa

E lectronic address: taw k@physik.uni-bielefeld.de

I. INTRODUCTION

The QCD phase diagram at nite temperatures and densities attracted increasing attention [1], especially as it became possible to perform lattice QCD simulations at nite baryo-chem ical potential $_{\rm B}$ [2, 3, 4, 5]. The numerical studies for the equation of state at nite $_{\rm B}$ provides a valuable framework for understanding the experimental signatures for the phase transition from conned hadrons to quark-gluon plasma (QGP). The heavy-ion experiments are aiming to explore the QCD phase diagram. Therefore, it is of great interest to show the interrelation between strangeness and baryo-chemical potentials and $T_{\rm c}$ in hadron resonance gas model (HRGM) compared with the available lattice QCD simulations.

It is known that QCD phase diagram has a very rich structure. From numerical simulations, we know that the location of the phase transition line depends on the quark masses and avors and the way of including the strange quark chemical potential $_{\rm S}$ at dierent values of $_{\rm B}$ and T. The isospin chemical potential can play an additional role. But relative to $_{\rm B}$ and $_{\rm S}$, the isospin chemical potential is very small, so that we can assume an entire symmetry in light quark potentials and therefore ignore the isospin chemical potential.

The rst point in QCD phase diagram, namely the point at T_c and = 0, has been a subject of dierent lattice simulations [2, 3, 4, 5, 6, 7, 8]. We know so far that for two quark avors ($n_f = 2$) the transition is second order or rapid crossover and the critical temperature is T_c 173 8 MeV. For $n_f = 3$, we have a rst order phase transition and T_c 154 8 MeV. For $n_f = 2 + 1$, i.e. two degenerate light quarks and one heavy strange quark, the transition is crossover and T_c 173 8 MeV. For the pure gauge theory, T_c 271 2 MeV and the deconnement phase transition is rst order.

The lattice QCD simulations at $_{\rm B}$ 6 0 is still lacking an elective exact algorithm and su er from the sign-problem. The ferm ion determinant gets complex and therefore the conventional Monte Carlo techniques are no longer applicable, since the lattice congurations can no longer be generated with the probability of the Boltzmann weight. However, during the last few years considerable progress has been made to overcome these problems [2, 3, 4, 5].

The signi cant numerical results on positioning the QCD phase diagram we have so far is that the transition line can be described by a parabola. The parabola can be viewed as a rejection of the truncations done in the Taylor expansions of different thermodynamic quantities calculated on lattice. In addition, we know from elective models such as bootstrap

and Nambu-Jona-Lasinio models that the structure of the phase diagram is complex. The freeze-out curve takes a much dierent behavior at large chemical potential [9, 10]. Nevertheless, one might think that for small chemical potential ($_{\rm q}$ T $_{\rm c}$) the curvature in the T $_{\rm c}$ -dependence upon $_{\rm q}$ can be tted as a parabola, where $_{\rm q}$ is the quark baryo-chemical potential. The situation at very large chemical potentials is not clear. One might need to take into account other eects, such as quantum elects at low temperatures [11, 12, 13, 14, 15, 16], which might be able to describe the change in the correlations from connect hadrons to coupled quark-pairs.

In present work, we take advantage of our previous work [17,18,19] on analysis the critical tem peratures T_c for dierent quark masses and on reproducing the lattice thermodynamics at zero and nite $_B$ by HRGM. We assumed that the deconnement is driven by a constant energy density. We have shown [17, 18] that the degrees of freedom rapidly increase at $_c$ (T_c ; $_B$ = 0). Here we assume that $_c$ remains constant along the whole phase transition line [19, 20], $_c$ (T_c ; 0) = $_c$ (T_c ; $_B$). Concretely, we propose that the existence of dierent transitions does not a ect the assumption that $_c$ is constant for all $_B$ -values. We have to emphasize here that it is not possible in the framework of this model to make any statement about the transition at very large $_B$ and low $_B$. The nature of the degrees of freedom in this region is very dierent from that of the nearly non-interacting QGP at high $_B$ and low $_B$. The message we have in this paper is that the condition driving the QCD phase transition at nite $_B$ and $_B$ [17, 18, 19] is the energy density. Its value is not a ected by the conjecture of existing of dierent transitions along the whole $_B$ -axis.

The model will be presented in Sec. II. In Sec. III, we introduce expressions for the lines of constant T_c . The lines of constant energy density are given in Sec. IV. The results are discussed in Sec. V. Sec. VI is devoted to the radius of convergence. In Sec. VII, we sum marize the conclusions.

II. THE MODEL

A ssum ing an ideal quantum gas consisting of point-like hadron resonances, the canonical partition function for one particle and its anti-particle reads

$$Z(V;T;) = g \frac{V}{2^{-2}} \int_{0}^{Z_{-1}} dk k^{2} \ln(1 + e^{(")+T}) + \ln(1 + e^{("+)+T});$$
 (1)

where stand for bosons and ferm ions, respectively. " = $(k^2 + m^2)^{1-2}$ is the single-particle energy and g is the spin-isospin degeneracy factor. Under the given assumptions, one can sum up the contributions from all resonances pieces, so that

$$\ln Z^{\text{(id)}}(V;T;) = \sum_{i}^{X^{2}} \ln Z_{i}(V;T;_{i}):$$
 (2)

In this expression, there are two important features included; the kinetic energies and the sum mation over all degrees of freedom and energies of resonances. On the other hand, we know that the formation of resonances can only be materialized through strong interactions [21]; Resonances (reballs) are composed of further resonances (reballs), which in turn consist of resonances (reballs) and so on.

In spite of this, if one would like to take into consideration all kinds of resonance interactions in HRGM, then, for instance, by means of the S-matrix, we can re-write Eq. (2) as an expansion of the fugacity term.

$$\ln Z^{(int)}(V;T;) = \ln Z^{(id)}(V;T;) + \sum_{i=2}^{X^d} a_i(T) \exp(-iT);$$
 (3)

S-m atrix describes the scattering processes in the therm odynam ical system [22]. a (T) are the so-called virial coe cients and the subscript refers to the order of the multiple-particle interactions.

a (T) =
$$\frac{g_r}{2^3} \int_{M}^{Z_1} dw e^{(r_r(w))=T} X$$
 (21+ 1) $\frac{e}{e_w}$ 1(w):

The sum runs over the spatial waves. The phase shift $_1$ (w) of two-body inelastic interactions, for instance, depends on the resonance half-width $_r$, spin and mass of produced resonances,

$$\ln Z^{\text{(int)}}(V;T;) = \ln Z^{\text{(id)}}(V;T;) + \frac{g_r}{2^3} \int_{M}^{Z} dw \frac{e^{("_r(w) + r) = T}}{(M_r - w)^2 + \frac{r}{2}^2};$$
 (5)

By inserting in place of in Eq. (5), we take into consideration the two-particle inelastic interactions, from which the anti-particles will be produced. For narrow width and/or at low temperatures the virial term reduces, so that we will get the non-relativistic ideal

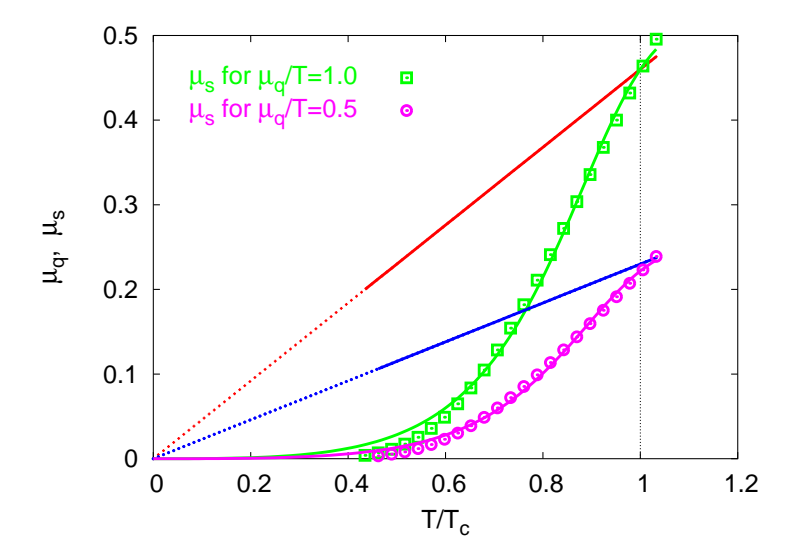


Fig. 1: The strange quark chem ical potential $_{\rm S}$ vs. ${\rm T}={\rm T}_{\rm C}$ for $_{\rm q}={\rm T}$ = 1 and $_{\rm q}={\rm T}$ = 0.5 (straight lines). The results are ted according to Eq. \emptyset). At ${\rm T}$ = 0, we not that $_{\rm q}=_{\rm S}=$ 0. As ${\rm T}$! ${\rm T}_{\rm C}$, the strangeness chem ical potential approaches the baryo-chem ical potential, $_{\rm S}=_{\rm q}$. The units used here are $^{\rm p}-_{\rm q}$ 420 M eV.

partition function of the hadron resonances with elective masses M . In other words, the resonance contributions to the partition function are the same as that of free particles with some elective mass. At temperatures comparable to $_{\rm r}$, the elective mass approaches the physical one. Thus, at high temperatures, the strong interactions are taken into consideration via including heavy resonances, Eq. (2). We therefore suggest to use the canonical partition function Eq. (2) without any corrections. Furthermore, we do not apply the excluded volume corrections. We include all hadron resonances with masses up to 2 GeV, such a way we avoid the singularities expected at Hagedom temperature [17, 18].

In the two sections which follow, we discuss how to include the strangeness chemical potential $_{\rm S}$ in HRGM and lattice QCD .

A. s in hadron resonance gas model

The hadron-based chemical potentials $_{\rm B}$; $_{\rm S}$ are related to the quark-based ones, $_{\rm q}$; $_{\rm S}$

$$S = 3 q; \qquad S = q S; \qquad (6)$$

A ssum ing that the isospin and charge chem ical potentials are vanishing, we use the following combination for the hadron resonances

$$= 3b_q + s_s; (7)$$

where b and s are the baryon and strange quantum numbers, respectively. Obviously, the quantum numbers are conserved in these expressions.

The initial conditions in heavy-ion collisions apparently include zero net strangeness. This is expected to remain the case during the whole interaction unless an asymmetry in the production of strange particles happens during the hadronization. As we are interested in the hadron thermodynamics and location of QCD phase transition, we suppose that the net strangeness is entirely vanishing. The average strange particle number reads

$$< n_s > = \frac{1}{N} \sum_{i=1}^{N} \frac{(i)}{s} \frac{e \ln Z^{(i)} (V;T;)}{e^{(i)}s}$$
: (8)

In Z is given in Eq. (3) and $_{\rm S}$ is given in Eq. (6). $_{\rm S}$ = exp ($_{\rm S}$ =T) is the fugacity factor of squark. The procedure used to calculate the quark-based $_{\rm S}$ is the following: For given T and $_{\rm Q}$ (or $_{\rm B}$), we iteratively increase $_{\rm S}$ starting from zero. In each iteration, we calculate the di erence < $n_{\rm S}$ > < $n_{\rm S}$ > , Eq. (8). The value of $_{\rm S}$ which disposes zero net strangeness is the one we read out and shall use in calculating the therm odynamic quantities. As in Eq. (6) the relation between $_{\rm S}$ and $_{\rm S}$ is given by taking into consideration the baryonic property of squark. The resulting $_{\rm S}$ for di erent $_{\rm Q}$ (or $_{\rm B}$) and T are depicted in Fig.1. From this numerical method, we t $_{\rm S}$ as a function of T and $_{\rm B}$,

$$s = \frac{0.138 \#^{-3}}{1 + 2.4 + 2.7 + 3}; \tag{9}$$

where # $_{\alpha}=T$ and $T=T_{c}$.

Let us note here that for these calculations we have re-scaled the resonance m asses in order to be comparable to the quark masses used in lattice QCD simulations. The procedure of giving unphysically heavy masses to the hadron resonances is introduced in [17, 18]. In these calculations, the mass of lightest Goldstone meson becomes $m = 770 \, \text{M}$ eV and consequently, the critical temperature gets almost as large as 200 MeV at $_{\text{B}} = 0$.

In order to guarantee vanishing net strange particle numbers in HRGM as the case in heavy-ion collisions, it is not enough to simply set $_{\rm S}=0$ and consequently, $_{\rm S}=_{\rm q}=_{\rm B}=3$ in Eq. (8). However, there are publications in which the authors have assigned $_{\rm S}$ to zero in

hadron matter and afferwards applied the G ibbs condition for the rst order phase transition to QGP. The reason is obvious. A side the baryons, the strange mesons with dierent contents of s quarks play determining roles at dierent temperatures and therefore, a ect the nal results, Eq. (6). Setting $_{\rm S}=0$, leads to violating the strange quantum numbers. Nevertheless, we will show here calculations in which we set $_{\rm S}=0$. We do this in order to extensively compare with lattice results. We apply this assignment in order to check the ability of HRGM in reproducing the current lattice simulations [20]. After accomplishing this successfully, we can go beyond the lattice constrains to show the physical picture. We will make predictions for QCD phase diagram for physical masses and non-truncated expressions. These predictions are to be confined by heavy-ion experiments and future lattice calculations with very small lattice spacing and physical quark masses.

For completeness of the discussion, we recall the situation in the plasma regime (see also next section). For conserving strangeness at $T > T_c$, we have to suppose that $_S = 0$. $_S$ consists of one baryonic part $_B = 3$ and another part coming from the strangeness quantum number $_S$. From Eq. (6), we then get

$$_{s} = _{q} = _{B} = 3:$$
 (10)

This result is con rmed in Fig. 1. For $_{\rm q}$ = 0 (or $_{\rm B}$ = 0), we not that $_{\rm s}$ = 0 for all temperatures. $_{\rm s}$ increases with increasing $_{\rm q}$ and T. At $_{\rm c}$, we not that $_{\rm q}$ $_{\rm s}$. Therefore, we can suggest to set $_{\rm q}$ = $_{\rm s}$ for all temperatures above $_{\rm c}$.

We can so far sum marize that $_{\rm S}$ in the hadron matter has to be calculated in dependence on $_{\rm B}$ and T under the assumption that the net strangeness is vanishing. In the QGP phase, one might full this assumption by setting $_{\rm S} = _{\rm B} = 3$. As we will see later, in lattice simulations, one assigns $_{\rm S} = _{\rm S} = 0$. We deal with all these cases in this work.

B . s in lattice Q C D

In the Euclidian path integral formulation, the partition function of lattice Q CD at $\ nite$ T and $\ reads$

$$Z (T;) = Tre^{(H N)=T}$$

$$= D D D A e^{S_f(V;T;)+S_g(V;T)}; \qquad (11)$$

where (;) and A are the ferm ion and gauge elds, respectively. The chem ical potential is given in Eq. (7). By Legendre transform ation of the H am iltonian H, we get the Euclidian action $S = \begin{bmatrix} R_{1-T} & R \\ 0 & dt \end{bmatrix}_V d^3xL$. The ferm ionic action is

$$S_f = a^3$$
 $ma_{x} + \frac{1}{2} X^4$ $ma_{x+\hat{k}} + a_{x+\hat{k}} + a_{x+\hat{k}}$ (12)

where a is the lattice spacing. As given in Eq. (8), the number density of the quarks with avor number x is obtained by derivation with respect to $_{x}$,

$$n_{x} = \frac{0}{0} \ln Z \ (T; x);$$
 (13)

For checking the dependence of $_{\rm S}$ on $_{\rm q}$ and consequently on $_{\rm B}$, it is enough to approxim ate the ferm ionic part of lattice QCD Lagrangian for three quark avors as

To taken into account the conservation of the baryon and strange quantum numbers, the sum mation in last expression has to run over s quarks, too. By doing this, last term turns to be ($_{\rm q}$ $_{\rm s}$) $\rm n_{\rm s}$. Then we expect that the strangeness on lattice vanishes at $_{\rm s}$ = $_{\rm q}$. But from Eq. (14), which re ects the situation in current lattice simulations, we not that $\rm n_{\rm s}$ = 0 for $_{\rm s}$ = 0.

As discussed in previous section, the strangeness in QGP is conserved at $_{\rm S}=_{\rm q}=_{\rm B}=3$. In the hadron regime, especially at large $_{\rm B}$, $_{\rm S}$ (or $_{\rm S}$) has to be calculated as a function of T and $_{\rm B}$ (Fig. 1). In spite of these considerations, the reliable lattice QCD simulations are still limited to $_{\rm B}$ 3T_c. As we will see in Sec. V, at this small value, there is practically no big dierence between $_{\rm S}=0$ and $_{\rm S}=f(T;_{\rm B})$.

III. LINES OF CONSTANT Tc

A. $T_c($) in hadron resonance gas model

In Boltzmann limit, the energy density in an ideal quantum system consisting of one particle and its anti-particle can be expressed as

$$(T;) = \frac{g}{2} T m^2 m K_1 \frac{m}{T} + 3T K_2 \frac{m}{T} \cos \frac{1}{T}$$
 (15)

is given in Eq. (7). We can divide this expression into two sectors: one meson-m and one baryon-sector b [18, 23].

$$"_{h}(T;) = "_{m}(T) + "_{b}(T) \cosh(=T);$$
 (16)

Applying truncations in the Taylor expansions up to the second order of =T -as done in lattice calculations [24] -we can estimate the lines of constant T_c in HRGM. In doing this, we assume that "h (T;) = "h (Tc;0). Furthermore, we assume that the dependence of energy density on the quark mass is quite small. We see this in Fig. 2 which is reported in Ref. [25]. At T_c and for the same temporal lattice dimension N, there is very small change in "c for dierent quark masses. The latter are related to the pion masses via m 2 / mq.

The starting point in expressing $T_c(_B)$ for constant ratios $_B$ =T is to expand Eq. (16) around the points $T=T_c$ and $_B=0$. The second-order expansion gives

$$\mathbf{"}_{h} (T; _{B}) = \mathbf{"}_{h} (T_{c}; 0) + \frac{\theta \mathbf{"}_{h} (T_{c}; 0)}{\theta T} (T \quad T_{c}) + \frac{1}{2} \frac{2}{B} \frac{\theta^{2} \mathbf{"}_{b} (T_{c}; 0)}{\theta \frac{2}{B}};$$

$$= \mathbf{"}_{h} (T_{c}; 0) + \frac{\theta \mathbf{"}_{h} (T_{c}; 0)}{\theta T} (T \quad T_{c}) + \frac{1}{2} \mathbf{"}_{b} (T_{c}; 0) \frac{B}{T} ^{2} : (17)$$

Under the assumptions given above, this leads to the following parabola:

$$\frac{T_{c(B)}}{T_{c(B)}} = 1 \frac{9}{2} \frac{1}{T_{c(B)}} \frac{\| (T_{c}; 0) \|_{b}}{\frac{e}{eT} \|_{h} (T_{c}; 0)} \frac{q}{T};$$
 (18)

where $_{\rm q}$ = $_{\rm B}$ =3. In order to map out the QCD phase diagram by using this analytic expression, we merely need to calculate the baryon energy density $_{\rm b}$ at $T_{\rm c}$ and $_{\rm q}$ = 0 and the derivative of the hadron energy density with respect to T. The results are given in Sec. V. Evidently, it is possible to extend the above expression to include further higher terms of $_{\rm q}$ =T.

Then to determ ine T_c at given $_B$, we apply besides the above analytical method the condition of constant critical energy density [19, 20] (see Sec. IV). In this case, T_c is defined as the temperature at which the energy density in hadron resonance gas reaches a certain critical value. This value can be taken from lattice QCD simulations at $_B$ = 0.

B. $T_c()$ in lattice QCD

In lattice QCD simulations, the critical temperature $T_c()$ is to be calculated from the pseudo-critical coupling $_c()$ by determining the susceptibility peak in either the Polyakov loop or the chiral condensate in $\frac{1}{2}$ dimensions. The lattice beta function (a) which can be obtained from the string tension is needed in order to express the results in physical units. From the rst non-trivial Taylor coe cients of $T_c()$, we get

$$\frac{d^{2}}{d^{2}}T_{c}() = \frac{N^{2}}{T_{c}(=0)}\frac{e^{2}_{c}()}{e^{2}} a^{1}\frac{ea}{e};$$
 (19)

where N is the temporal lattice dimension.

In the lattice QCD simulations [4] with $n_f=2$ and quark m ass am $_q=0:1$, the dependence of T_c on $_q$ has been found to take the following (parabola) expression:

$$\frac{T_{c}(q)}{T_{c}(q=0)} = 1 \quad 0.070(35) \quad \frac{q}{T_{c}(q=0)} \quad (20)$$

In other lattice QCD simulations with the same avor number but quark masses four times heavier than the physical masses [3],

$$\frac{T_{c}(q)}{T_{c}(q=0)} = 1 \quad 0.050(34) \quad \frac{q}{T_{c}(q=0)} \quad (21)$$

It has been concluded [4] that the last relation remains almost unchanged for am $_{\rm q}=0.005$. In this regard, we have to remember that for small quark masses perturbative beta function has been used. As we will see later, we actually not an increase in the curvature with reducing resonance masses from the values which very well simulate the current lattice calculations (m 770 MeV) to the physical masses, at which the lightest Goldstone meson is the physical pion (m = 140 MeV).

The results from Eq. (20) are depicted in Fig. 3. In the same gure, we plot Eq. (21). We also plot other lattice results [4], namely the short vertical lines which give T_c at constant energy density.

 $n_f = 3$ lattice QCD results [26] for dierent quark masses obtained so far can be sum m arized as

$$\frac{T_{c}(q)}{T_{c}(q=0)} = 1 \quad 0.025(6) \quad \frac{q}{T_{c}(q=0)}^{2}; \quad \text{am } q = 0.1;$$

$$= 1 \quad 0.114(46) \quad \frac{q}{T_{c}(q=0)}^{2}; \quad \text{am } q = 0.005;$$
(22)

= 1 0:114 (46)
$$\frac{q}{T_{g}(q=0)}$$
; am $q=0:005$: (23)

A gain, in these simulations the beta function for the small quark masses has been calculated perturbatively. The results from these two expressions are depicted in Fig. 5 and Fig. 6, respectively. From other $n_f = 3$ lattice QCD simulations [27],

$$\frac{T_{c}(q)}{T_{c}(q=0)} = 1 \quad 0.0610(90) \quad \frac{q}{T}^{2} + 0.00235(89) \quad \frac{q}{T}^{4} : \tag{24}$$

The curvature from $\,n_f=2+1\,$ lattice $sim\,u\,$ lations [28] has been compared with the three avor one [3] and concluded that there is a complete agreem ent. As we will see in Fig. 6, the most recent $n_f = 2 + 1$ lattice simulations [29] result in a curvature smaller than those from other lattice simulations. This can be understood according to the di erent ferm ionic actions used.

IV. LINES OF CONSTANT ENERGY DENSITY

In previous work [19], we have used HRGM in order to determ ine T_c corresponding to a wide range of quark (pion) masses at $_{\rm B}$ = 0. The masses range from the chiral to pure gauge lim its. We have seen that the condition of constant energy density can excellently reproduce the critical temperature $T_{\rm c}$ as a function of m $_{\rm q}$ and $n_{\rm f}$. In present work, we extend this condition to nite chemical potentials. We use two models for including the strangeness chemical potential $_{\rm S}$. In the rst model, we calculate $_{\rm S}$ in dependence on $_{\rm B}$ and T according to the condition of zero net strangeness. In the other one, we explicitly set the quark-based s = 0. The last case is used in lattice QCD simulations. As given in Sec. IIB, the proper inclusion of $_{
m s}$ in QGP and in lattice Lagrangian is to assign to it the sam e value of $_{\rm B}$ = 3. Nevertheless, both choices can be accepted for the current lattice QCD simulations, since the most reliable lattice calculations have been performed at small baryo-chem ical potentials ($_{\rm q}$ $_{\rm T_c}$). Consequently, the strangeness chem ical potential is expected to be much small.

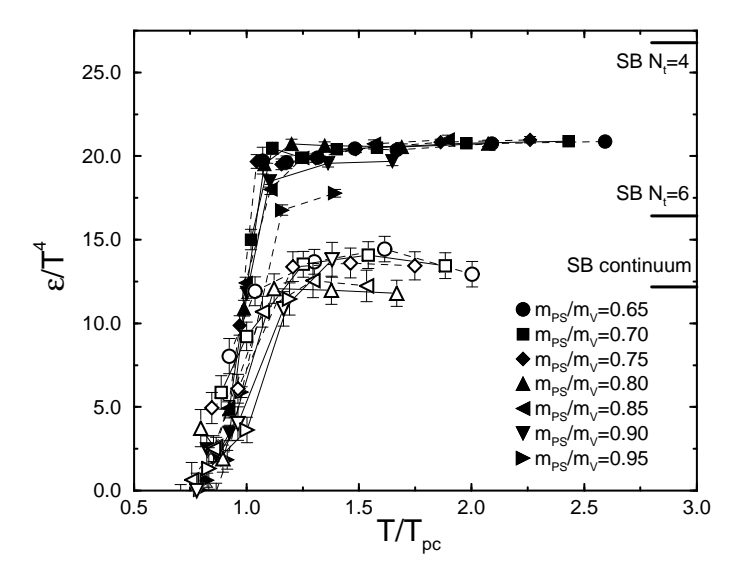


Fig. 2: The energy density normalized to T 4 given in dependence on T=T $_c$ for dierent quark masses m $_q$ and temporal lattice dimensions N 4 . This gure is reported in Ref. [25].

As discussed above, in HRGM, the energy density at nite chemical potential can be divided into two parts: one from the meson sector and another one from the baryon sector. For the rst part, we can completely drop out the fugacity term. For symmetric numbers of light quarks, the baryo-chemical potential of mesons is vanishing. But for strange mesons the strangeness chemical potential assigned to their squarks should be taken into account. For the baryon sector, the chemical potential is given by Eq. (7).

The question we intent to answer is: which value has to be assigned to the critical energy density? We recall the lattice QCD simulations. In Fig. 2, we see that the energy density [31] at T_c is not a singular function but can rather be dened at dierent critical values depending on n_f and m_q . The uncertainty in the energy density is therefore large. The critical energy density at which we dene $T_c(_B)$ is taken from the lattice QCD simulations at $_B=0$ [8]. In lattice units, the dimensionless energy densities for $n_f=2$ and 3 are "= $T^4j_c=4:5$ 2 and = 6:5 2, respectively. We drop out the errors in these quantities. We take an average value and recalculate it in the physical units. Then, $_c=600$ 300 MeV=fm³. We assume that this value is independent on m_q and remains constant on the whole $_B$ -axis.

V. THE RESULTS

Since we want to compare HRGM with lattice results [3,4], some details about the lattice simulations at $_{q}$ 6 0 are in order. Details about HRGM are partially given in present work. Extensive details are presented in Refs. [17, 18, 19]. In order to avoid the sign problem in lattice simulations [4], the derivatives of therm odynamic quantities with respect to $_{B}$ = 0 at the point T_{c} are 1st computed and then their Taylor expansion coecients in terms of nite $_{q}$ are calculated. The curvatures according to T_{c} ($_{B}$) and $_{c}$ ($_{B}$) are derived for dierent m_{q} . For instance for am $_{q}$ = 0.1, the corresponding pion mass in lattice units for n_{f} = 2 is am = 0.958 (2), where a = 0.271 (10) [8]. This leads to m = 773 MeV. Keeping these features in mind, we performed our calculations for physical and re-scaled resonance masses. In Fig. 3, we indicate that our results are coincide with the lattice ones. In Ref. [3], the lattice simulations are performed with an imaginary chemical potential for n_{f} = 2 staggered quarks. For m = m i, the sign problem is obviously no longer existing. Using analytic continuation of the truncated Taylor series, one can then go to real. The light quark mass is four times the physical mass. The location of m are presented by the short curves in Figs. 3, 4 and 6.

A. Results for two avors

From the canonical partition function Eq. (1), we can derive the energy density at n ite them ical potential 6 0 as

$$(T;) = T \frac{\text{@T ln Z (T;)}}{\text{Z }_{1}^{\text{@T}}} \quad \text{T ln Z (T;)} + \frac{\text{@T ln Z (T;)}}{\text{@}}$$

$$= \frac{g}{2^{2}} \quad k^{2} dk \frac{\text{"(k)}}{e^{\text{("(k)})} = T} 1$$
(25)

In the Boltzm ann lim it and by taking into consideration one particle and its anti-particle, we get the expression given in Eq. (15). It is obvious that the trigonometric function included in last expression are not truncated. In calculating this quantity in HRGM, we sum up over all resonances we take into account.

We rst start with two avors. It is not needed to care about the strangeness chemical potential. As discussed above, there are two lattice QCD simulations for $n_f=2$. In the rst one, re-weighting method, the physical quantities which usually can be calculated at

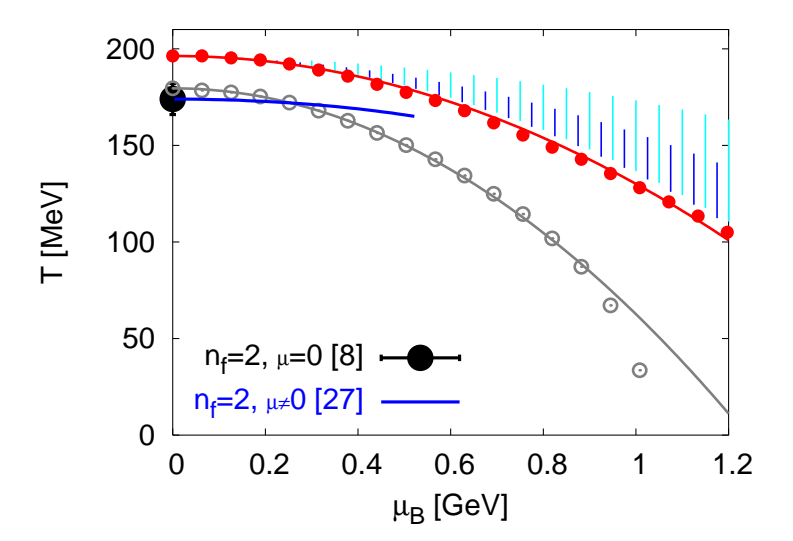


Fig. 3: T $_{\rm B}$ phase diagram for two quark avors ${\rm n_f}=2$. The vertical lines give the lattice results [4]. The short lines show the results according to a constant energy density. The long ones are for constant critical temperature. The Lattice simulations are performed for large quark mass. The corresponding Goldstone pion gets a mass of 770 MeV. The solid circles give our results heavy quark masses. The results for physical quark masses are given by the open circles.

 $_{\rm B}$ = 0 without any disculties have responses at nite $_{\rm B}$. The responses are utilized to estimate the thermodynamic quantities at nite $_{\rm B}$. The other lattice simulations [3] use imaginary $_{\rm B}$ and afterwards apply analytical continuation. At given $_{\rm B}$, $T_{\rm c}$ is determined as the temperature at which the energy density equals 600 MeV=fm³.

The results are plotted in Fig. 3. The solid circles represent the results for re-scaled resonance m asses. The open circles represent the results for physical m asses. The two lines connecting the points are obtained by ts according to:

$$\frac{T_{c}(q)}{T_{c}(q=0)} = 1 \quad C_{l} \quad \frac{q}{T_{c}(q=0)}$$
 (26)

The $_{\rm q}$ -values are restricted within the range 0 $_{\rm q}$ T $_{\rm c}$. $_{\rm q}$ is given in Eq. (6). For the re-scaled heavy m asses, the t parameters are c_1 = 0:115(36) and T $_{\rm c}$ ($_{\rm B}$ = 0) = 196:3 M eV . P lugging these parameters in Eq. (26), we get the top line in Fig. 3. The comparison with the lattice calculations Eq. (20) gives a satisfactory agreement, especially at low $_{\rm B}$. Nevertheless, it is obvious that our results at large $_{\rm B}$ lie below the lattice ones. The reason for this discrepancy will be discussed later.

As given above, the coe cient in the front of $(q=T)^2$ in Eq. (18) can be calculated in

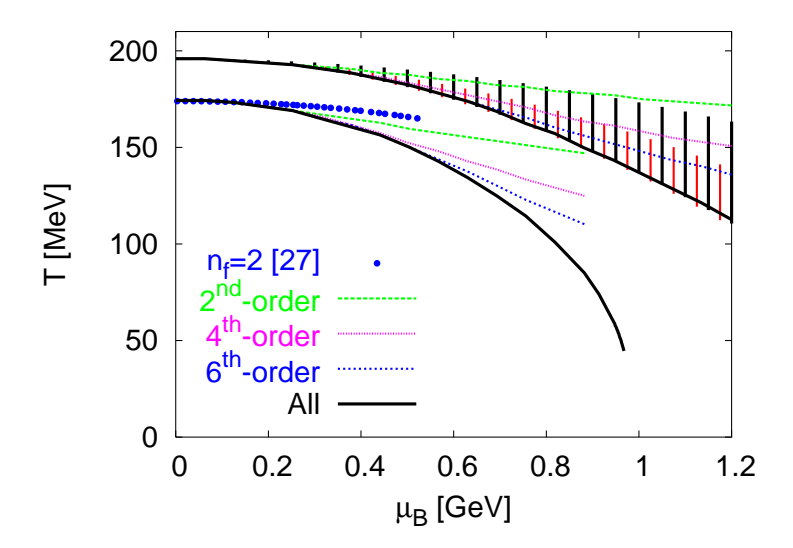


Fig. 4: The same as in Fig. 3. Here, we show the results obtained from the condition of constant energy density truncated up the dierent Taylor orders. The truncation is obviously able to describe the lattice QCD simulations for dierent quark masses [4, 27]. The solid lines give our predictions for non-truncated trigonom etric functions.

HRGM. For non-strange hadron resonances with re-scaled masses, the coe cient gets the value 0.0767. Com paring to Eq. (20), this value is obviously much better than the value of c_1 in describing the lattice results. As we will see, this discrepancy is to be related to the fact that c_1 has been calculated from thing T_c at nite $_B$ in the results which we have obtained from non-truncated (T; $_B$). We should emphasize that all Taylor terms that are higher than the second one are explicitly excluded in deriving Eq. (18). This partially explains the disagreem ent between HRGM and lattice results shown so far. We also study the case for physical resonance masses. The transmeters are $c_1 = 0.195$ (21) and T_c ($t_0 = 0$) = 175 MeV. The coe cient in Eq. (18) is found to be 0.1368.

In the following, we confront the lattice results with HRGM results which have been obtained from truncated expressions. We show the results in Fig. 4. We start with results from entire Taylor expansion for heavy resonance masses (solid line). This is equivalent to use Eq. (15) instead of Eq. (25). We note that this line shows almost the same behavior as that of the solid circles in Fig. 3. In deriving Eq. (15), the Boltzmann limit is assumed. The results from dierent truncations are also plotted. We note that the energy density truncated up to the second or fourth order of =T can describe the lattice results better

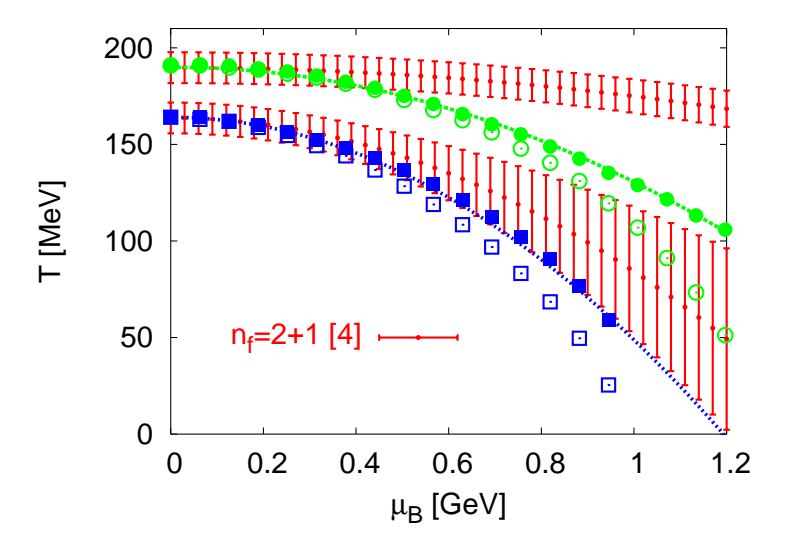


Fig. 5: The T $_{\rm B}$ phase diagram for ${\rm n_f}=3$. The vertical short lines represent the lattice results [4]. The above band corresponds to heavy quark masses. The bottom one is for physical masses. The solid circles are our results for heavy resonances and for $_{\rm S}=0$. The open circles are for $_{\rm S}={\rm f}(_{\rm B};{\rm T})$. The squares give the results for the physical masses. The curves are tted according to Eq. (26).

than the solid line. The agreement between the curvatures of these two lines and that from the analytical expression Eq. (18) is excellent. The ability of truncated expression to produce results comparable to the lattice ones is to be explained by the fact that the lattice results them selves have been obtained from truncated therm odynamic expressions.

We plot in the same gure HRGM results with physical masses. The curves obtained from dierent truncation terms in Eq. (15) represent our predictions when it will be possible to perform lattice simulations for two quark avors with physical masses. These predictions has to be checked by future lattice simulations. We note that the solid line is comparable to the bottom points plotted in Fig. 3. The quark masses used in Ref. [27] are relative heavy. Nevertheless, we see that the second order (dashed line) agrees very well with these lattice results [27] (solid circles).

B. Results for three avors

We have to include strangeness chem ical potential $_{\rm S}$ (Sec. IIA). Assuming that the three quarks are degenerate, we can use the same critical energy density as done in previous section. The results are shown in Fig. 5. The solid circles show the results for re-scaled

heavy resonance m asses. As done in lattice calculations, we set $_{\rm S}=0$. The resulting points (solid circles) are ted within the range 0 $_{\rm q}$ T $_{\rm c}$ according to Eq. (26). The t parameters are T $_{\rm c}=190$ M eV and c $_{\rm l}=0$:1016. The coe cient in front of (=T) 2 in Eq. (18) is 0:0505. C om paring with Eq. (22), this value can describe the lattice curvature much better than c $_{\rm l}$. We also calculate $_{\rm S}$ in dependence on $_{\rm B}$ and T assuming strangeness conservation. The open circles show the T $_{\rm C}$ $_{\rm B}$ diagram corresponding to this value of $_{\rm S}$. We note that the former case ($_{\rm S}=0$) is much closer to the lattice results than the latter one. The reason is, as we mentioned above, that $_{\rm S}$ in lattice calculations used to be assigned to zero.

The results for physical masses are also shown in Fig. 5. The solid squares represent the results at $_{\rm S}$ = 0. These points are tted according Eq. (26). The t parameters are $T_{\rm C}$ = 164 MeV and $c_{\rm I}$ = 0:17. The coe cient in Eq. (18) takes the value 0:1122, which agrees very well with Eq. (23). The open squares represent the results at $_{\rm S}$ that depends on $_{\rm B}$ and T. The results with re-scaled resonance masses are given as circles. For $_{\rm S}$ = 0, we get results closer to lattice results than for $_{\rm S}$ = f (T; $_{\rm B}$). In this gure, the energy density is calculated according to Eq. (25). In other words, the results plotted here are deduced from expression like Eq. (15), i.e. without any truncations.

We plot in Fig. 6 the results from dierent truncations, in order to compare HRGM results with lattice simulations. For heavy masses the results are given in the top panel. The results for physical masses are given in the bottom panel. It is clear that the truncation up to the second order gives results in a good agreement with the lattice simulations [4]. With higher truncations, we get curves with larger curvatures. We also plot two curves from non-truncated expressions. The solid curve is obtained by computing $_{\rm S}$ in dependence on T and $_{\rm B}$. O by iously, it is identical to the solid symbols plotted in Fig. 5. The dashed curve next to the solid one – shows the results in which $_{\rm S}$ is entirely vanishing. It gives the same behavior as that of the open symbols in Fig. 5.

We can so far conclude that the lattice results [4] can be reproduced by HRGM, if the trigonom etric functions are truncated in the same way. The lattice curvature within the region $$^{\circ}$$ T can excellently be described by HRGM .

In the bottom panel, we show other three avor lattice results. In Ref. [27], the numerical simulations have been performed with Wilson gauge action and three degenerate avors of staggered fermions. The quark masses are ranging between 0.025 am $_{\rm q}$ 0.04. It is clear that our results can reproduce the structure given by these data. We see that the curva-

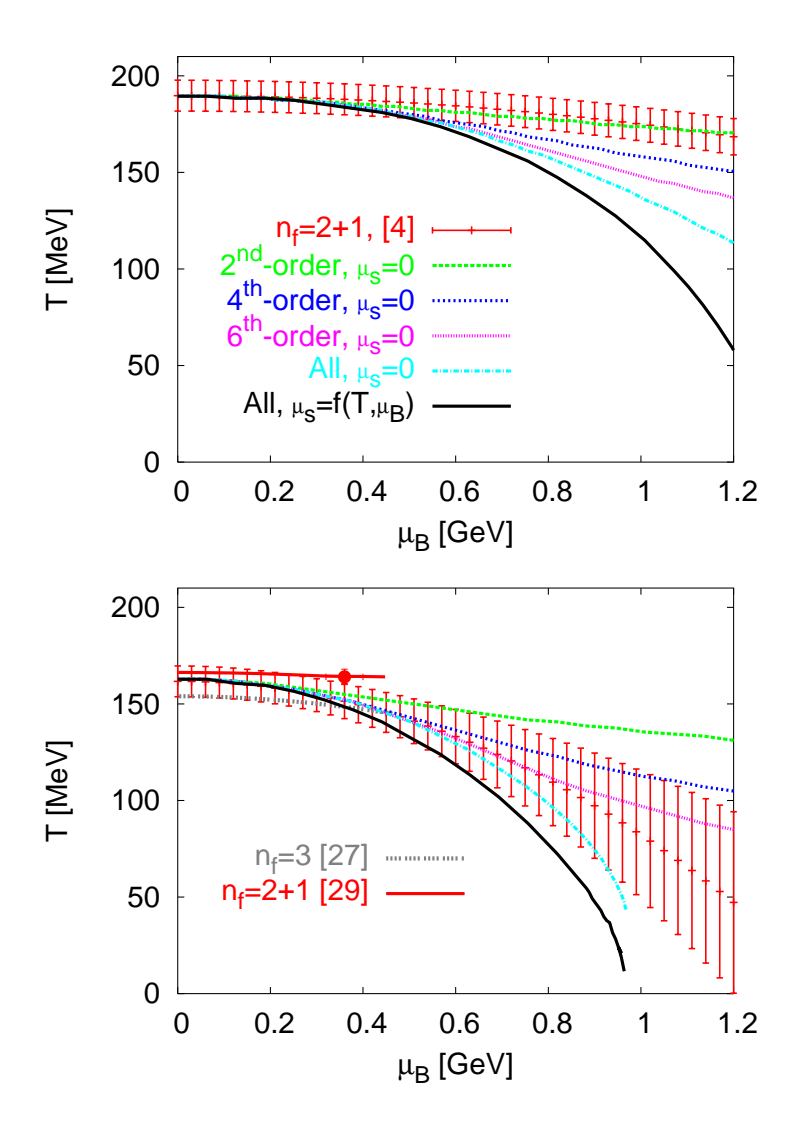


Fig. 6: T $_{\rm B}$ phase diagram as in Fig. 5. Here, we check the elects of truncated trigonom etric functions. The top panel shows the results for heavy masses. Truncating $(T;_{\rm B})$ up to second order reproduces the lattice results [4]. In the bottom panel we show the results with physical masses, the lattice results [4] are very well reproduced by the condition of truncating \cdot . The results from non-truncated at $_{\rm S}$ = 0 and $_{\rm S}$ = f (T; $_{\rm B}$) are also plotted. The agreement with the lattice simulations [27, 29] is also convincing

ture can be described by second or fourth order in HRGM . This is also valid for $n_f=2+1$ lattice results [29]. In this case, the quark masses am $_{u;d}=0.0092$ and am $_s=0.25$. Chiral extrapolations are done by heavier light quark masses. We also plot the latest calculations of the location of the endpoint. The endpoint in [30] lies at $_B=420\,\mathrm{M}$ eV . The corresponding temperature has not yet been calculated. The endpoint in [29] has the coordinates $_B=360-40\,\mathrm{M}$ eV and $_B=162-2\,\mathrm{M}$ eV . As discussed above, we assume that

the existence of endpoint does not a ect our results.

VI. RADIUS OF CONVERGENCE

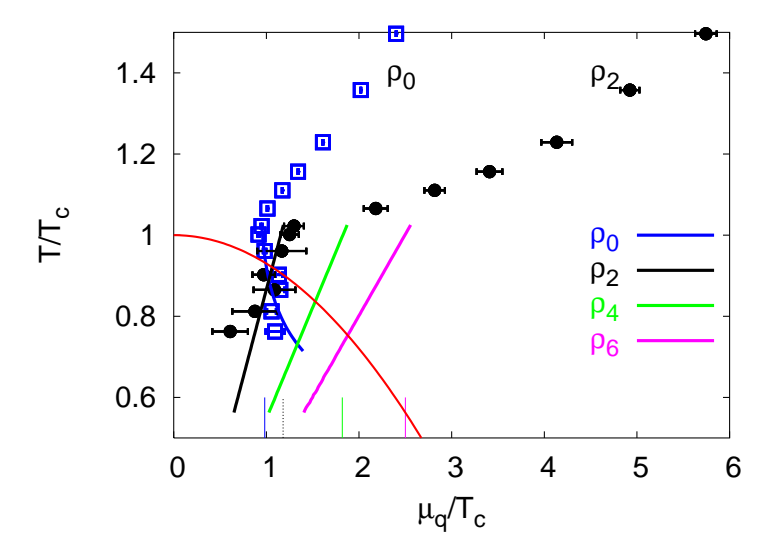


Fig. 7: Comparison between radii of convergence from the lattice [30] (points) and HRGM (lines). There is an excellent agreement with the existing lattice results. The T_c -curvature has been calculated by using lattice results with two avors (Fig. 3). The short vertical lines give the values of corresponding radii at T_c .

As we have seen, for a reliable comparison with the current lattice simulations, we have to apply truncations in the thermodynamic expressions in HRGM. Our objective here is to check the eciency of truncated series in locating the phase diagram. The radius of convergence rejects the singularity near T_c . It approaches unity near T_c . The energy density normalized to T^4 can be expressed as a trigonometric function depending on the ratio $T_c = T_c = T_c$. We use the property that the energy density is an even function in $T_c = T_c = T_c$ and therefore write

$$\frac{(T;_{B})}{T^{4}} = _{m}(T) + _{b}(T) \cosh \frac{B}{T}$$

$$_{b}(T) c_{2} \frac{q}{T}^{2} + c_{4} \frac{q}{T}^{4} ; \qquad (27)$$

where $c_n = (T_c = T)^n 3^n = n!$ and n is an even positive integer. The radius of convergence is

$$= \lim_{n!} \frac{C_n}{C_{n+2}}^{1=2} :$$
 (28)

In order to calculate the zero order radius, we recall the results at = 0 (not included in Eq. (27)).

$$_{\circ} = \frac{c_{0}}{c_{2}}^{1=2} = \frac{T}{T_{c}} \frac{2}{9} \frac{m (T)}{b (T; q = 0)} + 1$$

$$(29)$$

It is clear that $_0$ strongly depends on T. In Fig. 7, we not that close to T_c , $_0$ = 0.982, $_2$ = 1:18, $_4$ = 1:82 and $_6$ = 2.5. These values are shown as short vertical lines. The results agree very well with the available lattice results [B0]. As $_0$! 1, the radius of convergence approxim ately gives the lower bound for the critical endpoint ($_q$ T_c). This value exceeds the recent lattice results [24,29]. In principle, one expects that due to the absence of critical behavior in HRGM, the Taylor expansion Eq. (27) has an in nite convergence radius for all temperatures. At T_c and for = 1, one expects that the hadron degrees of freedom become indistinguishable from the degrees of freedom in QGP. In lattice simulations, the radii are bounded from above by the location of phase transition. Therefore, it is expected that the radii in Eq. (28) stay close to unity for T! T_c . In fact, this is the case in our low order one cients. The agreement between our results and the lattice ones is convincing. There are no published lattice results on the 6^{th} -order radius of divergence. Nevertheless, according to our expansion coelients, we expect that are steadily changing.

VII. CONCLUSIONS

We used HRGM to draw up T_c $_B$ diagram. The transition temperature T_c from hadronic matter to QGP has been determined according to a condition of constant energy density. Its value is taken from lattice QCD simulations at zero chemical potential and assumed to remain constant along the entire $_B$ -axis. We checked the in uence of squark chemical potential $_S$ on T_c . For including $_S$, we applied two models. In the rst one, we explicitly calculated $_S$ in dependence on T and $_B$ under the condition that the net strangeness vanishes. In the second one, we assigned, as the case in lattice QCD simulations, zero to $_S$ for all T and $_B$. The rst case, $_S$ = $f(T;_B)$, is of great interest for heavyion collisions. Furthermore, under this consideration, we expect that the strange quantum number is entirely conserved. This is not the case in the second model. Nevertheless, with the last assignment, the current lattice results are very well reproduced. On the other hand, one can apply the second model for current and future heavy-ion collisions. At BNL-RHIC and

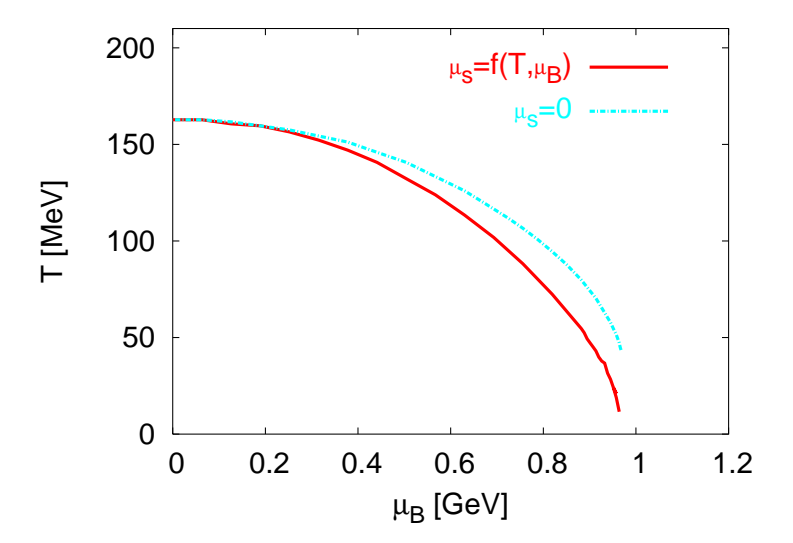


Fig. 8: Sum mary of our results on the QCD phase transition. In calculating both curves, we use all hadron resonances and suppose that the isospin chemical potential is vanishing. To obtain the top curve, we assigned $_{\rm S}$ to zero. $_{\rm S}$ is calculated in dependence on T and $_{\rm B}$. The results are given by the bottom curve. We note that both curves will cross the abscissa at the point of normal nuclear density.

CERN-LHC energies, for instance, $_{\rm B}$ (and consequently $_{\rm S}$) is very small. We have shown that the proper condition that guarantees vanishing strangeness in QGP is to set $_{\rm S}=_{\rm q}$. We did not check this explicitly. But it is obvious that $T_{\rm c}(_{\rm B}$; $_{\rm S}=0)$ quantitatively is not very much dierent from $T_{\rm c}(_{\rm B}$; $_{\rm S}$ (T; $_{\rm B}$)) at small $_{\rm B}$.

We have taken into consideration all hadron resonances given in particle data booklet with masses up to 2 GeV. For a reliable comparison with lattice, we have re-scaled the resonance masses to be comparable to the quark masses used in lattice simulations. With excluding the strange resonances, we compared our results with $n_f=2$ lattice results. With including all resonances, we reproduced $n_f=2+1$ lattice results. We note that increasing and seads to monotonic decrease in T_c . The results from HRGM match very well with the lattice simulations, especially within the sealest from the lattice calculations are most reliable ($_B=T$) $3T_c$. The agreement turns to be excellent, when we take into consideration the truncations done in calculating the thermodynamical quantity .

Besides this excellent agreement in the indirect calculation of T_c via constant energy density, we found that the analytical expression of T_c () up to the second order of (=T) greatly reproduced the curvatures calculated on lattice for dierent quark masses and avor

num bers.

Fig. 8 sum marizes our conclusions. The QCD phase diagram is plotted for a system including light as well as strange quarks. The Taylor expansion of energy density is not truncated. The two curves represents our predictions, when it will be possible to perform lattice simulations for physical masses and without the need to truncate the Taylor expansion. As T! 0, we note that both curves will cross the abscissa at almost one point. It is obvious that this point is corresponding to the normal nuclear density. The latter is related to $_{\rm B}$ 0:979GeV. The nature of the phase transition at very low temperatures does not lie within the scope of this work. However, there are many indications that the transition at T=0 occurs according to modication in the particle correlations. Changing the correlation leads to quantum phenomena, like quantum entropy [11, 12, 13, 14, 15, 16]. We also note that by switching on $_{\rm S}$ an increase in $T_{\rm C}$ is expected. At small $_{\rm B}$, the two curves are coincide.

A cknow ledgm ents

We gratefully acknowledge the useful discussions with David Blaschke, Frithjof Karsch, Berndt Muller, Krzsyztof Redlich and Boris Tomasik.

- [1] K.Rajagopaland F.Wilczek (2000), hep-ph/0011333.
- [2] Z.Fodor and S.D.K atz, Phys. Lett. B 534, 87 (2002), hep-lat/0104001.
- [3] P. de Forcrand and O. Philipsen, Nucl. Phys. B 642, 290 (2002), hep-lat/0205016.
- [4] C.R.Allton et al., Phys.Rev.D 66, 074507 (2002), hep-lat/0204010.
- [5] M.D'Elia and M.P. Lombardo, Phys. Rev. D 67, 014505 (2003), hep-lat/0209146.
- [6] R.V.Gavaiand S.Gupta, Phys.Rev.D 68, 034506 (2003), hep-lat/0303013.
- [7] F.Karsch, Lect. Notes Phys. 583, 209 (2002), hep-lat/0106019.
- [8] F.Karsch, E.Laermann, and A.Peikert, Nucl. Phys. B 605, 579 (2001), hep-lat/0012023.
- [9] A.Taw k (2004), hep-ph/0410329.
- [10] A. Taw k (2004), hep-ph/0410392.
- [11] D.E.M iller and A. Taw k (2003), hep-ph/0308192.

- [12] D.E.M iller and A.Taw k (2003), hep-ph/0309139.
- [13] D.E.M iller and A. Taw k (2003), hep-ph/0312368.
- [14] D.E.M iller and A.Taw k, J.Phys.G 30, 731 (2004), hep-ph/0402296.
- [15] S. Ham ieh and A. Taw k (2004), hep-ph/0404246.
- [16] D.E.Miller and A.Taw k, Acta Phys. Polon. B 35, 2165 (2004), hep-ph/0405175.
- [17] F. Karsch, K. Redlich, and A. Taw k, Phys. Lett. B 571, 67 (2003), hep-ph/0306208.
- [18] F.Karsch, K.Redlich, and A.Taw k, Eur. Phys. J. C 29, 549 (2003), hep-ph/0303108.
- [19] K.Redlich, F.Karsch, and A.Taw k, J.Phys.G 30, S1271 (2004), nucl-th/0404009.
- [20] D. Toublan and J.B. Kogut (2004), hep-ph/0409310.
- [21] R. Hagedom, Nuovo Cim. Suppl. 3, 147 (1965).
- [22] R.Dashen, S.-k.Ma, and H.J.Bernstein, Phys. Rev. 187, 345 (1969).
- [23] F.Karsch, Prog. Theor. Phys. Suppl. 153, 106 (2004), hep-lat/0401031.
- [24] S.E jiri et al., Prog. Theor. Phys. Suppl. 153, 118 (2004), hep-lat/0312006.
- [25] A.AliKhan et al. (CP-PACS), Phys. Rev. D 64, 074510 (2001), hep-lat/0103028.
- [26] F. Karsch et al., Nucl. Phys. Proc. Suppl. 129, 614 (2004), hep-lat/0309116.
- [27] P. de Forcrand and O. Philipsen, Nucl. Phys. B 673, 170 (2003), hep-lat/0307020.
- [28] Z.Fodor, Nucl. Phys. A 715, 319 (2003), hep-lat/0209101.
- [29] Z.Fodor and S.D.Katz, JHEP 04,050 (2004), hep-lat/0402006.
- [30] C.R.Allton et al., Phys.Rev.D 68, 014507 (2003), hep-lat/0305007.
- [31] Com paring fullQCD with pure gauge results, we get a feeling about the dependence of critical values on quark mass. $_{\rm c}$ =T 4 seem to be dierent, but with taking into consideration the dierent critical temperatures, we not that the $_{\rm c}$ are comparable with each other.